

# High Strength Shear Reinforcement (HIDEC 685H)

Toshiya KAWAHARA<sup>\*1</sup>  
Rippo KAWAI<sup>\*1</sup>

Takashige NAGATO<sup>\*1</sup>

## Abstract

*High strength shear reinforcement HIDEC 685H was developed for steel reinforced concrete construction and has a minimum of 685 N/mm<sup>2</sup> (7,000 kgf/cm<sup>2</sup>) of yield strength. The material used is a deformed coil reinforcement. Applying in-line heat treatment with hot water as coolant after the rolling mill, the material has less carbon amounts despite the high strength shear steel reinforcement and it has good weldability. This paper reports on the development of materials for HIDEC 685H and procedures for designing of concrete construction.*

## 1. Introduction

The increasing sophistication of building technology and the change in the living environment in urban areas in recent years have encouraged the construction of many high-rise buildings of reinforced concrete (RC) construction. To obtain sufficient strength and toughness in RC members subjected to large shear forces, it is often difficult to provide a necessary amount of shear reinforcement by use of conventional carbon steel reinforcing bars with a yield strength of 295 N/mm<sup>2</sup>. The damage to buildings and other structures in the Great Hanshin Earthquake of January 17, 1995 suggests that still higher strength and toughness are required of RC members. Against these backgrounds, the shear reinforcement steel HIDEC 685H with a minimum yield strength of 685 N/mm<sup>2</sup> can be applied as shear reinforcement to enable the economical design of RC members.

This report gives an overview of the material development of the HIDEC 685H manufactured at the Muroran Works, presents the results of experiments conducted to evaluate the shear strength of RC members made using the HIDEC 685H as shear reinforcement, and describes the RC member design methods verified according to the experimental results.

## 2. High-Strength Coil Reinforcement for Shear Reinforcement

### 2.1 Required properties

Shear reinforcement is required to have high strength and toughness in combination, good weldability when welding closed hoops, and appropriate rib shape that does not impair dimensional

accuracy when bending bars into various forms. The HIDEC 685H aimed at a minimum 0.2% offset yield strength of 685 N/mm<sup>2</sup> to achieve a short-term allowable stress of 585 N/mm<sup>2</sup> (6,000 kgf/cm<sup>2</sup>). The minimum elongation was set at 8% according to the transverse reinforcement steel USD785 standardized in the Ministry of Construction's comprehensive technology development project "Development of technology for construction of ultra-lightweight and ultrahigh-rise reinforced concrete buildings". The steel development history and the ideas exploited to attain these properties are described below.

### 2.2 Steel manufacturing process and composition

In the high-strength wire rod manufacturing process, controlled cooling is often employed after hot rolling. The wire rod mill of the Muroran Works has various types of controlled cooling equipment, including blast-air cooling, cold- and hot-water immersion cooling, and retarded cooling with cover. To obtain a high-strength wire rod as the starting material for the HIDEC 685H, it was decided to use a hot-water controlled cooling facility with boiling water as a coolant. The chemical composition of steel was developed on the basis of the manufacturing technology of the high-strength wire rod steel<sup>1)</sup> developed for bolts and pre-stressed concrete (PC) wire, in order to stably obtain a bainite microstructure at the cooling rate of the hot-water cooling equipment.

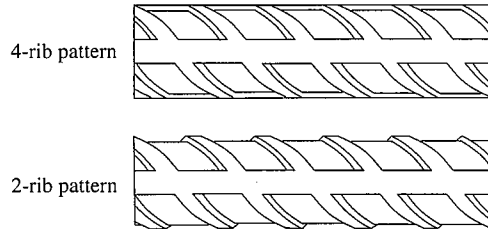
The basic chemical composition of the HIDEC 685H is given in Table 1. The cooling process is relatively high in the cooling rate, so that the addition of carbon and other alloying elements and the thickness of scale that affects weldability can be reduced. The addition of carbon can be reduced by utilizing precipitation strengthening and solid-solution strengthening with the trace addition of special alloying elements. Generally, increasing the carbon

<sup>\*1</sup> Muroran Works

**Table 1 Chemical compositions (mass%) of HIDE C 685H**

C	Si	Mn	P	S	Cu	Special elements	Carbon equivalent
< 0.20	< 1.20	< 2.00	< 0.030	< 0.025	< 0.10	Added	< 0.70

$$\text{Carbon equivalent (\%)} = \text{C} + \text{Mn}/6 + \text{Si}/24 + \text{Ni}/40 + \text{Cr}/5 + \text{Mo}/4 + \text{V}/14$$

**Fig. 1 Rib patterns of HIDE C 685H**

content of a steel makes the steel more difficult to weld. The HIDE C 685H has such a low carbon content that it can be easily welded by the flash butt welding process, among other welding processes.

### 2.3 Bendability

The HIDE C 685H has ribs specified in JIS G 3112, Steel bars

**Table 2 List of beam specimens**

Fracture type	Number	$F_c$ (kgf/cm <sup>2</sup> )	Shear span-to-depth ratio (M/QD)	$p_w$ (%)	$p_t$ (main reinforcement ratio) (%)
Shear fracture type	24	210	1.0	0.254	3.00(5-D'25)
	25			0.424	
	26			0.794	
	16		1.5	0.254	
	17			0.424	
	18			0.794	
	5	360	2.0	0.254	D': Main reinforcement diameter
	6			0.424	
	7			0.794	
	27		1.0	0.753	
	19			1.179	
	8			1.179	
	28	360	1.0	0.75	0.98(7-D'13)
	20			1.18	
	9			1.18	
	29		1.5	0.406	
	22			0.203	
	13			0.406	
Bending fracture type	3	210	2.0	0.406	1.27(3-D'22)
	10	360		0.219	
	11	360		0.316	
	4	210		0.530	
	12	360	2.5	0.318	1.66(5-D'19)
	1	210		0.636	
	2	360		0.373	
				0.373	
				0.373	
				0.373	

for concrete reinforcement, in order to ensure sufficient bond with concrete. Since the shape of the ribs has an effect on the dimensional accuracy of bent reinforcing bars, the HIDE C 685H has "oblique ribs"<sup>2)</sup> designed to reduce the variation in the bending dimensions. Bars with four ribs can also be made to reduce the dimensional variation further. Fig. 1 shows the rib patterns of the HIDE C 685H. The HIDE C 685H is fabricated into a variety of forms, such as squares, circles, and polygonal hoops and spiral reinforcement. The adoption of oblique ribs provides fabricated reinforcement with good dimensional accuracy.

## 3. Bending Shear Experiments

### 3.1 General

#### 3.1.1 Specimens

Beam and column specimens are listed in Tables 2 and 3, respectively. Twenty-one specimens of the beam shear fracture type, nine specimens of the beam bending fracture type, and 24 specimens of the column shear fracture type, or 54 specimens in total were prepared. The beam specimens were all 225 mm by 450 mm in the section, and the column specimens were all 400 mm by 400 mm in the section. The shape and bar arrangement of the beam and column specimens are shown in Figs. 2 and 3, respectively. The design strength of concrete,  $F_c$ , was set at two levels of 210 and 360 kgf/cm<sup>2</sup> for both beam and column specimens. The shear span-to-depth ratio M/QD (where M is the bending moment, Q is the shear force, and D is the member cross-sectional depth, beam or column depth) was set at three levels of 1.0, 1.5 and 2.0 for the shear fracture type and at three levels of 1.5, 2.0 and 2.5 for the bending fracture type. The shear reinforcement ratio  $p_w$  was

**Table 3 List of column specimens**

Fracture type	Number	Axial stress	$F_c$ (kgf/cm <sup>2</sup> )	Shear span-to-depth ratio (M/QD)	$p_w$ (%)	$p_t$ (main reinforcement ratio) (%)
Shear fracture type	1	$F_c/6$	360	1.0	0.357	1.81(5-D'25)
	2				0.422	
	3				0.792	
	4				1.100	
	5				0.253	
	6				0.422	
	7	$F_c/3$	210	1.5	0.792	2.53(7-D'25)
	8				0.143	
	9				0.238	
	10				0.357	
	11				0.422	
	12				0.422	
	13	$F_c/6$	360	2.0	0.422	1.81(5-D'25)
	14				0.422	
	15				0.422	
	16				0.357	
	17				0.422	
	18				0.792	
	19	$F_c/3$	210	1.5	0.422	2.53(7-D'25)
	20				0.792	
	21				0.238	
	22				0.422	
	23				0.422	
	24				0.422	

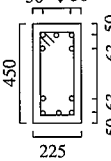
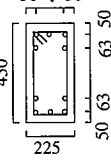
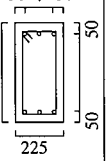
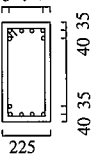
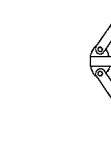
Fracture type	Shear fracture type	Bending fracture type			
Beam tension main reinforcement	5-D'25	5-D'19	5-D'22	3-D'22	7-D'13
Cross section (mm)	Loading direction 50 ↓ 50 	Loading direction 50 ↓ 50 	Loading direction 50 ↓ 50 	Loading direction 50 ↓ 50 	Loading direction 35 ↓ 35 

Fig. 2 Shape and bar arrangement of beam specimens

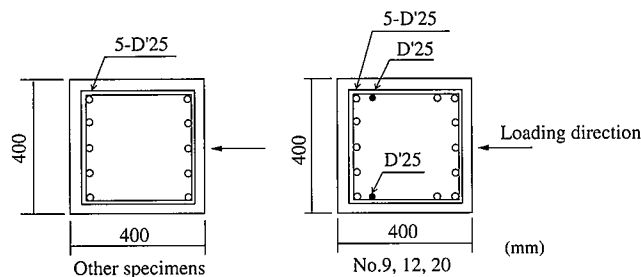


Fig. 3 Shape and bar arrangement of column specimens

set in the range of 0.254 to 1.179% for the beam shear fracture type, in the range of 0.219 to 0.636% for the beam bending fracture type, and in the range of 0.238 to 1.10% for the column shear fracture type.

### 3.1.2 Loading and measuring methods

The loading apparatus of the column specimens is illustrated in Fig. 4. The loading method developed by the Building Research Institute, Ministry of Construction was adopted. The horizontal force was applied to the specimen with a 100-ton oil jack, and the axial force was applied to the specimen with a 200-ton oil jack. The load was repeatedly applied with gradually increasing displacement. The member rotational angle was varied in the range of  $1/800$  to  $1/75$ . The relative displacement of the upper and lower stubs was measured in four positions, or left, right, top surface, and bottom surface, as shown in Fig. 5.

### 3.2 Experimental results

The experimental results<sup>3)</sup> of the beam specimens are described below.

#### 3.2.1 Crack and fracture conditions

Fig. 6 shows the crack and fracture conditions of beam specimens at the end of the experiment. The shear fracture type and the bending fracture type both developed bending cracks at the left and right ends immediately after loading. Bending shear cracks and shear cracks then occurred in the range of  $1.5D$  ( $D$  is the beam depth) from each beam end. Some of the specimens of the shear fracture type with low concrete strength exhibited bond splitting fracture. The experimental data were utilized for evaluating the reliable shear strength equations that take the effect of bond splitting fracture into account. For the bending fracture type, shear fracture and bond splitting fracture were both observed as the fracture modes responsible for the loss of strength after flexural yielding.

#### 3.2.2 Load-deformation relationship

Fig. 7 shows load-deformation curves of beam specimens. The shear fracture type decreased in strength with increasing displacement

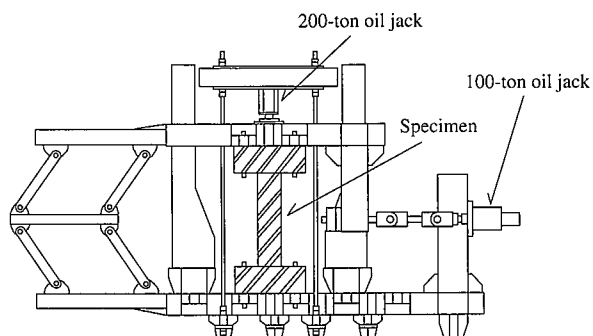


Fig. 4 Loading apparatus of column specimens

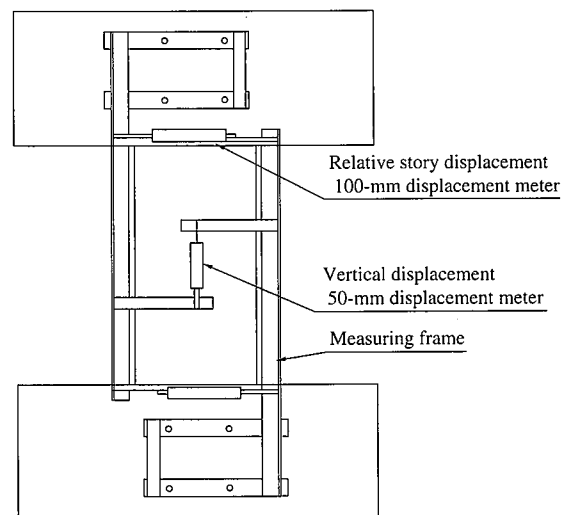


Fig. 5 Displacement measuring procedure

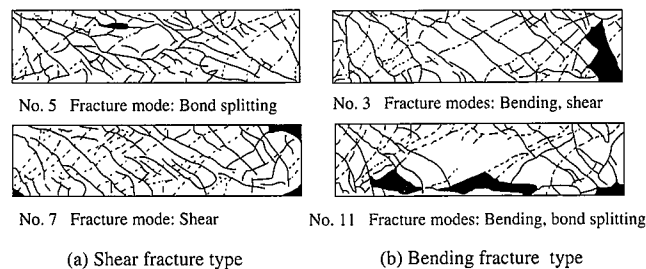


Fig. 6 Crack and fracture conditions of beam specimens

ment amplitude after the maximum strength, and exhibited more brittle fracture characteristics as the shear reinforcement ratio increased. The bending fracture type increased in maximum strength with increasing concrete strength, was small in the amount of deformation at the maximum strength, and exhibited brittle fracture characteristics.

#### 3.2.3 Deformation capacity of beam bending fracture type

The rotational angle of a member at which the strength of the member is reduced to 80% of its maximum strength on the load-deformation envelope is defined as the critical deformation angle. Fig. 8 shows the relationship between the measured critical deformation angle and the hinge rotational angle calculated as specified in the "Design Guidelines for Earthquake Resistant Reinforced

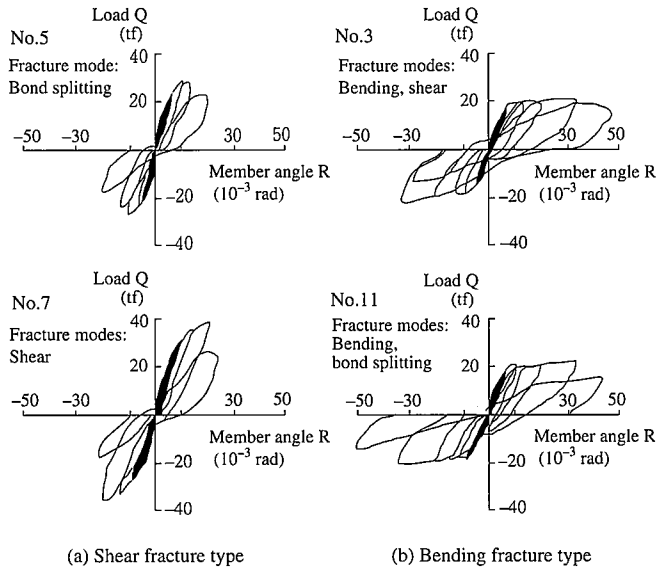


Fig. 7 Load-deformation curves of beam specimens

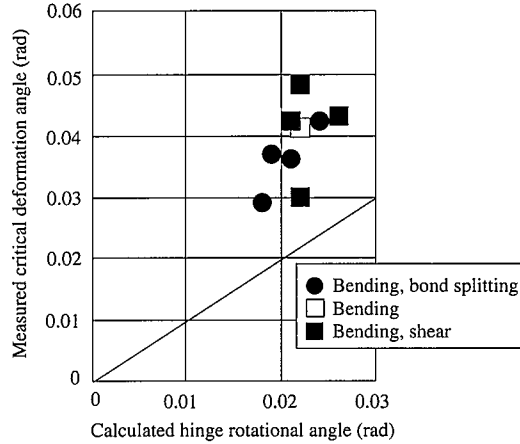


Fig. 8 Relationship between measured and calculated hinge rotational angle

Concrete Buildings Based on Inelastic Displacement Concept (Draft)" (hereinafter referred to as the inelastic displacement guideline)<sup>4)</sup>. All measured values excel the calculated values, indicating evaluation on the safe side.

## 4. Design Methods

### 4.1 Allowable shear strength

The second term of Eq. (1) for calculating the short-term allowable shear force of reinforced concrete members in the "Standard for Structural Calculation of Reinforced Concrete Structures" (hereinafter referred to as the RC standard)<sup>5)</sup> was changed from  $(p_w - 0.002)$  to  $(p_w - 0.001)$  by considering the strength of reinforcement. As a result, the short-term allowable shear strength  $Q_{AS}$  was calculated using the following equations:

For beams,

$$Q_{AS} = \{\alpha \cdot f_s + 0.5 \cdot f_t (p_w - 0.001)\} b \cdot j \quad (1)$$

For columns,

$$Q_{AS} = \{f_s + 0.5 \cdot f_t (p_w - 0.001)\} b \cdot j \quad (2)$$

where,

$$\alpha : 4/(M/QD + 1)$$

$f_s$  : Allowable shear stress of concrete

$f_t$  : Allowable tensile stress of HIDEDEC 685H (585 N/mm<sup>2</sup>)

$b$  : Width of beam or column

$p_w$  : Shear reinforcement ratio

$j$  : Lever arm,  $j = (7/8)d$

$d$  : Effective depth of beam or column

The shear reinforcement ratio  $p_w$  is 0.2% or more and is set at 0.6% if it exceeds 0.6%.

The relationship between the measured ultimate strength and the calculated short-term allowable shear force of the beam and column specimens is shown in Fig. 9. The average safety factor (ultimate strength/short-term allowable shear force) is 1.54 for the beam specimens and 1.92 for the column specimens, which means that the beam and column specimens are both on the safe side.

The reinforcing effect of the shear reinforcement of the beam and column specimens made using the HIDEDEC 685H is shown in Figs. 10 and 11, respectively. To evaluate the shear reinforcement effect, the shear force carried by the concrete in the beam is denoted by  $\alpha \cdot f_s$  ( $f_s$  for the column) as specified in the RC standard. The deduction of this shear force portion from the measured ultimate strength  $\tau_u (= Q_{exp}/b \cdot j$  where  $Q_{exp}$  is the measured ultimate shear stress) yields the shear reinforcement contribution. The measured values are fully on the safe side with respect to the calculated values for both the beam and column specimens.

### 4.2 Ultimate shear strength

The ultimate strength  $V_u$  to be used in secondary design is the smallest of the values calculated by Eqs. (3) to (5). These equations are the same as the reliable shear strength equations adopted in the inelastic displacement guideline.

$$V_u = \mu p_{we} \sigma_{wy} b_e j_e + \{v \sigma_B - 5 p_{we} \sigma_{wy} / \lambda\} b D \tan \theta / 2 \quad (3)$$

$$V_u = (\lambda \sigma_B + p_{we} \sigma_{wy}) b_e j_e / 3 \quad (4)$$

$$V_u = \lambda v \sigma_B b_e j_e / 2 \quad (5)$$

where,

$\mu$  : Factor indicating angle of truss mechanism

$p_{we}$  : Effective shear reinforcement ratio

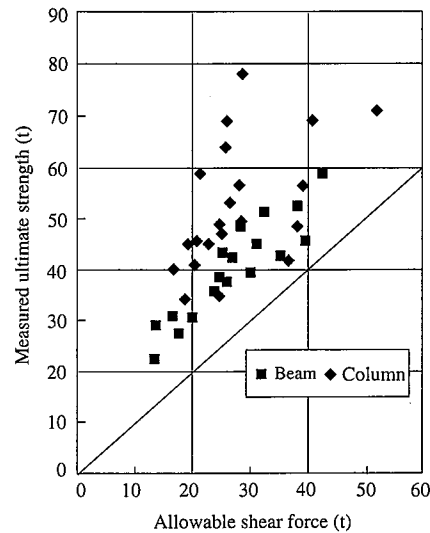


Fig. 9 Relationship between measured ultimate strength and calculated short-term allowable shear force

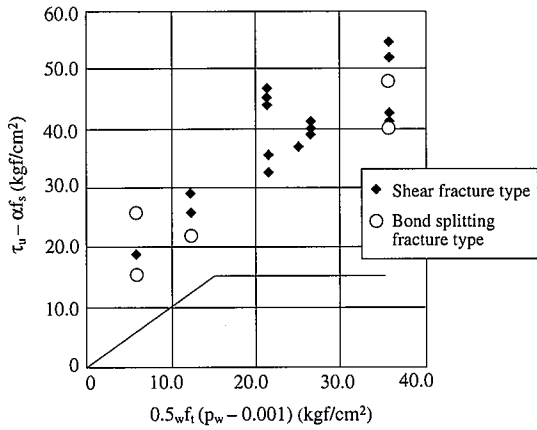


Fig. 10 Reinforcing effect of shear reinforcement of beam specimens

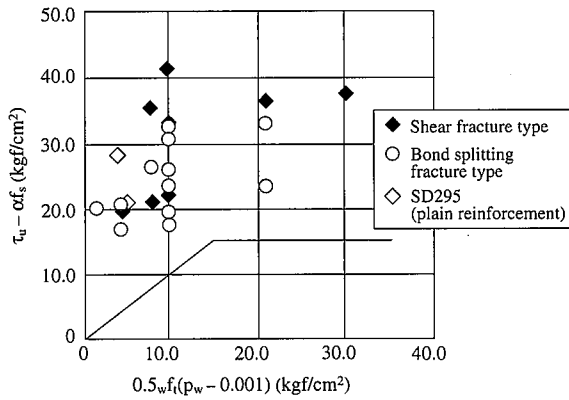


Fig. 11 Reinforcing effect of shear reinforcement of column specimens

$\sigma_{wy}$  : Strength (685 N/mm<sup>2</sup>) of HIDE6 685H for ultimate shear strength

$b_e$  : Effective width of member section

$j_e$  : Effective depth of member section

$v$  : Effective factor for compressive strength of concrete

$\sigma_B$  : Compressive strength of concrete

$\lambda$  : Effective factor for truss mechanism

$\theta$  : Angle of compression member in arch mechanism

Figs. 12 and 13 show the relationship between the measured ultimate strength and the ultimate strength calculated by Eqs. (3) to (5) for the beam and column specimens of the shear fracture type, respectively. The measured values were all larger than the calculated values for both the beam and column specimens. The average measured/calculated value ratio was 1.158 (coefficient of variation of 7.6%) for the beam specimens and 1.164 (coefficient of variation of 9.4%) for the column specimens. According to these results, it was decided to adopt the equations given in the inelastic displacement guideline for calculating the ultimate shear strength of the HIDE6 685H.

#### 4.3 Design for bond

The shear reliability strength  $V_{bu}$  that takes the effect of bond splitting fracture into account is the smallest of the values calculated using Eqs. (6) and (7). Equations (6) and (7) are the same as those adopted in the inelastic displacement guideline.

$$V_{bu} = \sum(\tau_{bu}\psi) j_e + \{v\sigma_B - 2.5\sum(\tau_{bu}\psi) / \lambda b_e\} b D \tan \theta / 2 \quad (6)$$

$$V_{bu} = \lambda v \sigma_B b_e j_e / 2 \quad (7)$$

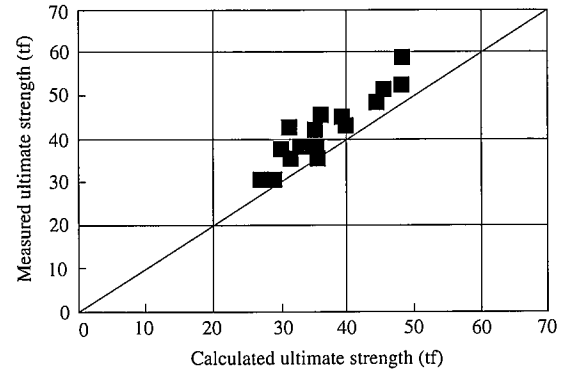


Fig. 12 Relationship between measured and calculated ultimate strength of beam specimens

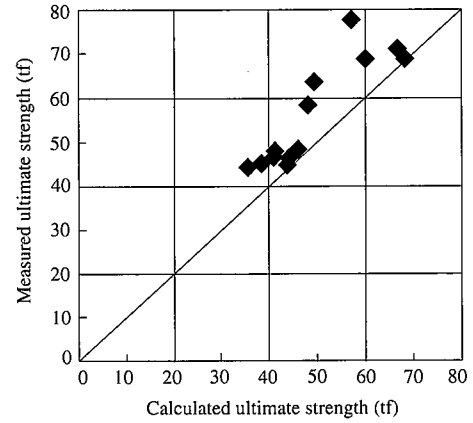


Fig. 13 Relationship between measured and calculated ultimate strength of column specimens

where,

$$\sum(\tau_{bu}\psi) = \tau_{bu}\sum\psi_1 + \tau_{bu2}\sum\psi_2$$

(for member designed as yield hinge)

$$= (1 - 10R_p) \tau_{bu}\sum\psi_1 + \tau_{bu2}\sum\psi_2$$

(for member not designed as yield hinge)

$\tau_{bu}$  : Bond reliability strength of first-tier main reinforcement  
 $\sum\psi_1$  : Total circumferential length of first-tier main reinforcement

$\tau_{bu2}$  : Bond reliability strength of second-tier main reinforcement  
 $\sum\psi_2$  : Total circumferential length of second-tier main reinforcement

$R_p$  : Rotational angle in hinge region in ultimate limit state

The bond strength derived on the basis of the equation proposed by Fujii and Morita is adopted in the "Design Guidelines for Earthquake-Resistant Reinforced Concrete Buildings Based on Ultimate Strength Concept" (hereinafter referred to as the ultimate strength guideline)<sup>6)</sup>. Recent research, however, has pointed out that the equation underestimates the bond splitting strength of members in which secondary shear reinforcement is placed. A bond splitting strength equation that appropriately evaluates the effect of secondary shear reinforcement on the basis of many experimental results about bond strength in recent years and that is relatively high in accuracy is adopted in the inelastic displacement guideline.

Fig. 14 shows the relationship between the measured ultimate strength and the ultimate strength calculated by Eqs. (6) and (7) for the beam specimens. Since only three beam specimens failed

by bond splitting, the data of the beam specimens that failed by shear were included in Fig. 14. The second-tier main reinforcement is incorporated into the calculated ultimate strength data. Fig. 15 shows the relationship between the measured and calculated ultimate strength of the column specimens. The data of the column specimens are entirely those of the column specimens that failed by bond splitting. The second-tier main reinforcement is not incorporated into the calculated ultimate strength data. The measured values were all larger than the calculated values for both beam and column specimens. The average measured/calculated value ratio was 1.144 for the beam specimens and 1.155 for the column specimens. According to these results, it was decided to adopt the equations specified in the inelastic displacement guidelines for calculating the shear reliability strength that takes the bond splitting fracture effect of the HIDEDEC 685H into account.

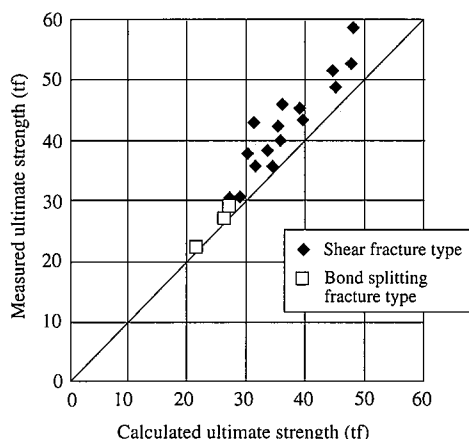


Fig. 14 Relationship between measured and calculated ultimate strength of beam specimens

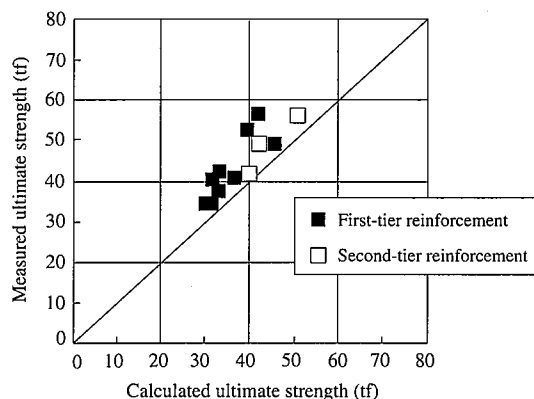


Fig. 15 Relationship between measured and calculated ultimate strength of column specimens

## 5. Conclusions

The design methods for safely and efficiently evaluating the high-strength shear reinforcement steel HIDEDEC 685H with a minimum yield strength of 685 N/mm<sup>2</sup> has been verified. More specifically,

- 1) In-line heat-treated high-strength coil reinforcement has been developed by finely adjusting the chemical composition of low-carbon bainite steel and employing hot-water controlled cooling equipment.
- 2) The validity of allowable stress design using the allowable shear force equations specified in the RC standard has been verified.
- 3) The validity of ultimate strength design using the shear reliability equations specified in the inelastic displacement guideline has been verified.
- 4) The validity of bond design using the shear reliability equations that are specified in the inelastic displacement guideline and that take bond fracture into account has been verified.

## Acknowledgments

The authors would like to thank Professor Takuji Shibata (presently President) and Assistant Professor Hiroshi Takeda of the Hokkaido Institute of Technology for their guidance in the overall performance evaluation of the HIDEDEC 685H. They are also indebted to Professor Yasuyuki Arai and his students at the Muroran Institute of Technology for cooperation in beam specimen experimentation and data reduction.

## References

- 1) Gondo, H. et al.: Seitetsu Kenkyu. (303), 75(1980)
- 2) Daimaruya, M. et al.: J. JSTP. 37(428), 945(1996)
- 3) Kawahara, T. et al.: Shear Reinforced Effect of RC Beams Using High Strength Shear Reinforcement with a Minimum Yield Strength of 600 N/mm<sup>2</sup>. Hokkaido Branch of Architectural Institute of Japan, 1997
- 4) Architectural Institute of Japan: Design Guidelines for Earthquake Resistant Reinforced Concrete Buildings Based on Inelastic Displacement Concept (Draft). 1997.7
- 5) Architectural Institute of Japan: Standard for Structural Calculation of Reinforced Concrete Structures. 1994.2
- 6) Architectural Institute of Japan: Design Guidelines for Earthquake-Resistant Reinforced Concrete Buildings Based on Ultimate Strength Concept. 1990.11